Applied Polymer WILEY

DOI: 10.1002/app.51781

ARTICLE



Check for updates

Cyclization kinetics of gel-spun polyacrylonitrile/ aldaric-acid sugars using the isoconversional approach

Debjyoti Banerjee¹ | Hannah Dedmon¹ | Farzin Rahmani² | Melissa Pasquinelli² | Ericka Ford^{1,3}

Correspondence

Debjyoti Banerjee and Ericka Ford, Department of Textile Engineering, Chemistry and Science, Wilson College of Textiles, North Carolina State University, Raleigh, NC 27606, USA. Email: dbanerj4@ncsu.edu and enford@ncsu.edu

Funding information

Chancellor's Innovation Fund, North Carolina State University

Abstract

Comonomers, such as methacrylic acid, itaconic acid, and acrylic acid, can minimize the activation energy of polyacrylonitrile (PAN) cyclization through their nucleophilic reaction with pendant nitrile groups. An understanding of how these comonomers affect the kinetics of PAN cyclization inspired this study on how the isomeric sugars (glucaric acid(cis) and mucic acid(trans)) would influence PAN cyclization. Until now, researchers have characterized the cyclization of PAN by single activation energy; however, this approach using differential scanning calorimetry does not represent the conversion dependent kinetics of cyclization. The isoconversional method was used to evaluate exotherms for cyclization at three different heating rates while allowing the calculation of activation energy at incremental increases in conversion (α) . The aldaric acid sugars reduced the activation energy of initiation by ~five times in comparison to values observed for neat PAN fiber and the ratio of (k_1/k_2) (where k_1 is the rate constant for initiation and k_2 is the rate constant for propagation) improved by ~2 orders of magnitude. Based on molecular dynamic simulations, hydrogen bonding between the aldaric acids sugars and PAN lowered the activation energy at the onset of cyclization.

KEYWORDS

differential scanning calorimetry, extrusion, fibers, kinetics, thermal properties

1 | INTRODUCTION

With the increasing demands for carbon fiber (CF), polyacrylonitrile (PAN) has been the leading CF precursor-dominating more than 90% of the commercial market. The remaining 10% of CF precursors are made of petroleum-derived pitch and viscose rayon. Greater demands for CF have fueled research on how to improve the efficiency of CF production in terms of energy usage, production costs, and the physical properties of CF. A report by the Oak Ridge National Lab² shows that 40% of

the cost for PAN-based CF comes from processes of stabilization, oxidation, and carbonization. Of this, 65% of the energy requirement comes from stabilization and oxidation. High-strength CF production is commonly achieved through a series of steps that include the stabilization of precursor fiber in the air at temperatures <400°C, followed by carbonization under an inert atmosphere at ~350–1700°C, and finally graphitization under inert atmosphere at >2000°C). Understandably, stabilization is the first step toward the production of high-quality CF; herein, cyclization occurs between adjacent acrylonitrile

¹Department of Textile Engineering, Chemistry and Science, Wilson College of Textiles, North Carolina State University, Raleigh, North Carolina, USA

²Department of Forest Biomaterials, College of Natural Resources, North Carolina State University, Raleigh, North Carolina, USA

³The Nonwovens Institute, Wilson College of Textiles, North Carolina State University, Raleigh, North Carolina, USA

(AN) monomers under inert conditions. Cyclization is a key structural transformation within the overall scheme of stabilization, as it is a major stepping stone toward the development of graphitic carbon. It is important to note that cyclization does not require air to occur, but rather elevated temperatures under inert conditions or in the presence of air.

To evaluate and compare processes of PAN cyclization among emerging technologies for CF, a thorough study on the reaction kinetics of said precursors is imperative. The kinetics of PAN cyclization has been evaluated under isothermal or non-isothermal conditions. A single exotherm for PAN cyclization under non-isothermal conditions is needed for applying a standard model-based approach while multiple non-isothermal scans are recorded to evaluate using the model-free Kissinger method.³ While understanding the kinetics using Fourier transform infrared analysis (FTIR). Noh et al.4 treated samples isothermally at 170, 200, and 220°C, respectively for various intervals of time, and subsequently, the absorbance decay for the nitrile peak under FTIR was recorded. Initially, researchers proposed first-order kinetics to describe the cyclization of PAN-based precursor fibers, as measured by using differential scanning calorimetry (DSC) and FTIR.3-5 However, deviations from the first-order kinetic model were observed. FTIR was used by Collins et al. to study the kinetics of PAN fibers treated in air. The study revealed dual first-order reaction kinetics. This observation illustrates how a single firstorder kinetic model may not describe cyclization in its entirety.6 Both isothermal and non-isothermal DSC scans were used to evaluate the stabilization kinetics of PAN homopolymer and copolymer by Hay et al. Belyaev et al. also applied a model-fitting approach to DSC exotherms to evaluate the kinetic parameters for PAN terpolymer.⁸ Recently, Liu et al. evaluated the kinetics of PAN and PAN/softwood lignin fibers using the Kissinger method, which is based on the rate-dependent peak temperature and conversion for PAN exotherms.9 In addition, Moskowitz et al. 10 used the Kissinger method of evaluation of rate kinetics based on peak temperature to evaluate the activation energies of PAN-based copolymers with guanidium itaconate.

The model-fitting approach forcibly fits experimental data, which can generate ambiguous results. ¹¹ Furthermore, full conversion of a thermal process may not involve a single-step reaction model, but rather result from a sequence of multiple steps, each having its reaction model. Such multi-step reaction models should not be characterized by a single kinetic triplet, that is, fixed activation energy (E), fixed pre-exponential factor (A), and a definite reaction model $(f(\alpha))$. ¹² On the contrary, the model-free isoconversional method is a one-of-a-kind

approach that evaluates the kinetics of reactions based on the principle that reaction rate is a function of temperature-dependent conversion as defined by Vyazovkin in 2006.¹³ This method does not assume any reaction model before the evaluation of activation energy (E), but rather conversion-dependent values of activation energy (E_a) are used to define the reaction model (f[a]). Friedman, 1964,¹⁴ Flynn et al.,¹⁵ Ozawa,¹⁶ and Kissinger¹⁷ are some of the most notable initial works made in this domain. The isoconversional approach was used by Mishra et al. in 2014 to evaluate the kinetics of rice straw pyrolysis, 18 by Jankovic et al. in 2007 to characterize the dehydration of swollen poly(acrylic acid) hydrogels, 19 and by Hu et al. in 2018 to study the combustion of coal.20 However, its usage to understand the kinetics of PAN-based cyclization was missing until this work.

PAN homopolymer is highly pseudo-crystalline. The polar bonding between nitrile groups causes the strong bonding between the intermolecular chains. This often leads to challenges in dissolving the homopolymer in a suitable solvent. The slow dissolution of PAN homopolymer in solvents and localization of rapid heating from free-radical stabilization make PAN homopolymer an undesirable choice for CF.²¹ Further, the activation energy for PAN cyclization among fibers derived from homopolymer is high. The state-of-the-art for tailoring PAN cyclization focuses on the incorporation of ionic comonomers at up to 5% acrylonitrile (AN). The comonomers, having carboxylic acid groups, are capable of nucleophilic reaction with nitrile groups. For example, itaconic acid (IA) is a bio-based comonomer; methacrylic acid (MAA) and acrylic acid (AA) as synthetic comonomers. The advantages of using these comonomers are that each helps to minimize the evolution of heat while initiating the onset of cyclization at lower temperatures; thereby, reducing the activation energy barrier for cyclization.²² Common PAN comonomers have carboxylic acid groups that can initiate cyclization at elevated temperatures. 3,22,23 Inspired by this concept, we analyze the effect of diacid sugars (glucaric acid [GA] and mucic acid [MA]) as biobased initiators in the place of nucleophilic comonomers. The GA (cis) and MA (trans) isomers were gel spun within PAN-based fibers to supple the reaction of PAN cyclization.

This article is the first to provide a comparison of the non-isothermal kinetics of gel-spun PAN fibers with and without the 6-membered (*cis* or *trans*) diacid sugars. The isoconversional approach was used to identify mechanisms relevant to cyclization over the entire extent of conversion. For all cases, PAN having a low comonomer polymerization of 0.5% MAA was used. The isoconversional approach was used to evaluate the temperature and conversion-dependent activation energy for each system while being able to characterize cyclization.

2 | EXPERIMENTAL METHODS

2.1 | Materials

Polyacrylonitrile-co-MAA with 0.5 mol% MAAs (230 kDa, from Goodfellow) was used to make the PAN fibers. High purity GA termed *cis* (from Kalion Inc.) and MA (98% purity) termed *trans* (from Alfa Aesar) are modeled in Figure 2 along with images of atactic PAN. Acetone (>99.5% purity), isopropyl alcohol (99.9% vol/vol) and DMSO (99.9% purity) were supplied by Fisher Scientific. De-ionized water was sourced in-house.

2.2 | Gel-spun fiber processing

The *cis* and *trans* additives were weighed at 3.5 wt % to the mass of PAN (7.5 g). The solids were dissolved in 50 ml of DMSO at 85°C under stirring for 16 h to make a homogenous polymer solution. Subsequently, the gel spinning was performed using a 22-gauge needle (ID: 0.134 mm²) and a high-pressure spinning system. The coagulation bath comprised a 2:1:1 mixture of water/acetone/isopropyl alcohol, while the temperature of the bath was maintained around 10°C. The as-spun fibers underwent a single stage of thermal drawing at 140–160°C through oil. PAN fibers without additives were denoted as PAN, while fibers containing additives were denoted as PAN/*cis* and PAN/*trans*. Figure 1 shows the schematic of the gel-spinning process.

2.3 | Characterization of fiber morphology

The characterization of fiber morphology was performed using the Phenom G1 desktop scanning electron microscope (SEM) at 10 kV. Longitudinal mounts and cross-

sections of the fibers were sputter-coated using Gold Platinum mix on the Quorum Technologies SC7620 Mini Sputter Coater before imaging. To obtain fiber cross-sections, bundles of fiber were strung through a cork that was thinly sliced with a sharp blade. Assuming circular cross-sections, the effective diameter of fibers was evaluated using the ImageJ software for image processing.

2.4 | Wide-angle X-ray diffraction of fiber microstructure

The wide-angle X-ray diffraction of semi-crystalline PAN fibers was performed using the Rigaku SmartLab X-Ray Diffractometer at an operating voltage of 20–40 kV, with a current of 2–44 mA, using copper K_{α} X-rays (having a wavelength ' λ of $\lambda=0.154$ nm), and using the Soller slit for 1-D equatorial scans. Origin Pro 8.5 was used to analyze the WAXD patterns. Baselines were subtracted from the raw data and the patterns were normalized according to Equation (1),²⁴

Normalized intensity
$$(I) = \frac{i_n}{\sum_{n=1}^{\infty} i} \times 100$$
 (1)

where normalized intensity (I) is the ratio of each intensity at 2θ (i_n) divided by the sum of all diffraction intensities over the entire range of 2θ . The degree of crystallinity for all three samples was calculated by Equation (2),

$$\label{eq:decomposition} \begin{split} & \text{Degree of crystallinity (\%)} = \\ & \frac{\text{Area of the crystalline peaks}}{\text{Area of crystalline peaks} + \text{Area of amorphous peaks}} \times 100 \end{split}$$

The interplanar spacings of indexed diffraction planes (also known as d-spacings or *d*) were calculated

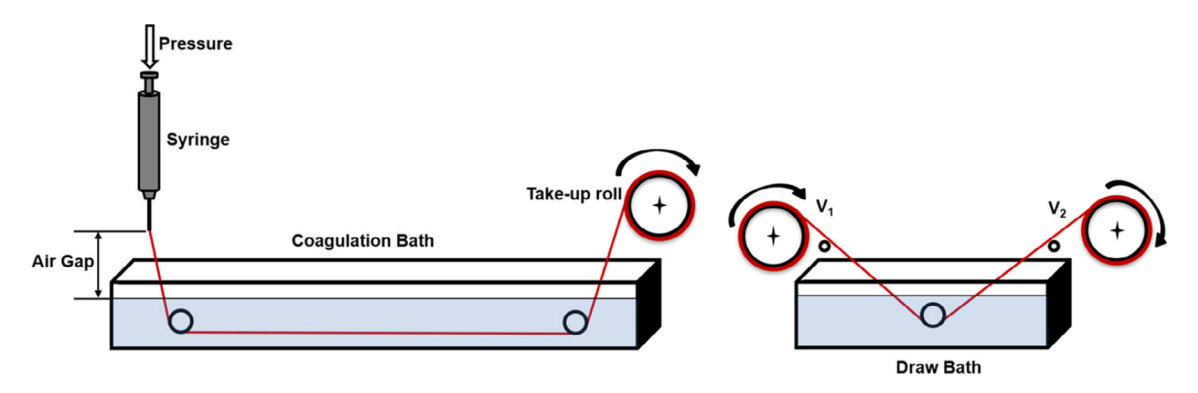


FIGURE 1 Single filament gel-spinning schematic of PAN, PAN/cis, and PAN/trans fibers [Color figure can be viewed at wileyonlinelibrary.com]

according to Bragg's law in Equation (3), where n = 1 for first-order reflections.

$$n\lambda = 2d \times \sin\theta \tag{3}$$

The average crystallite size along the [200] diffraction plane was calculated using Scherrer's equation (see Equation 4), where " τ " is average crystallite size, " β " is the FWHM of the [200] peak, and "k" is the dimensionless shape factor having a value of 0.9.

$$\tau = \frac{k\lambda}{\beta \cos \theta} \tag{4}$$

2.5 | Differential scanning calorimetry

Kinetic studies using DSC were performed on the TA Instruments Q2000 under an inert nitrogen atmosphere. Heating rates for kinetic analysis were 5, 10, and 20°C/min over 20–400°C. Also, the mass of samples used for DSC ranged from 5 to 7 mg.

2.6 | Molecular dynamics simulation

Molecular dynamics (MD) simulations were carried out to investigate the effect of aldaric acid isomers on the structure of PAN. The initial structure of each PAN/isomer

system was created using an amorphous builder within the Scienomics Materials and Processes Simulations (MAPS) platform Version 4.2.0 (compiled on the 21st of July in 2018). In this study, atactic polymer chains comprised of 100 AN repeating units. The initial structure of the PAN system and the chemical structures of cis and trans aldaric acids are shown in Figure 2. As systems were created in MAPS, the MD simulations were performed using the all-atomic DREIDING force field²⁵ within the LAMMPS software package (from March 31, 2017 by Sandia National Laboratories and distributed under the GNU Public License). In this work, the cut-off distance was 12 Å while the long-range electrostatic interactions were calculated using the particle-particle particle-mesh (PPPM) method.²⁶ The conjugate gradient method was used to perform geometry optimization. Once the systems relaxed, the MD simulation was carried out at 1000 K and atmospheric pressure for 3 ns. Then, the temperature of the systems gradually decreased from 1000 to 300 K at a rate of 0.7 K/ps with NPT simulation. Finally, the NPT simulation was performed to equilibrate the systems at 300 K and 1 atm for 1 ns. This heating/cooling cycle was repeated five times. For every 1000 AN-mers along the PAN chain, there were nine molecules of either the -cis or -trans molecule. The final average densities for PAN, PAN/cis, and PAN/trans were 0.960, 0.958, and 0.973 g/cm³, respectively. The aim of this work was to provide molecular level insight into the polymer and additive complexes in the solid state and to describe the molecular arrangements that may aid the onset of PAN cyclization.

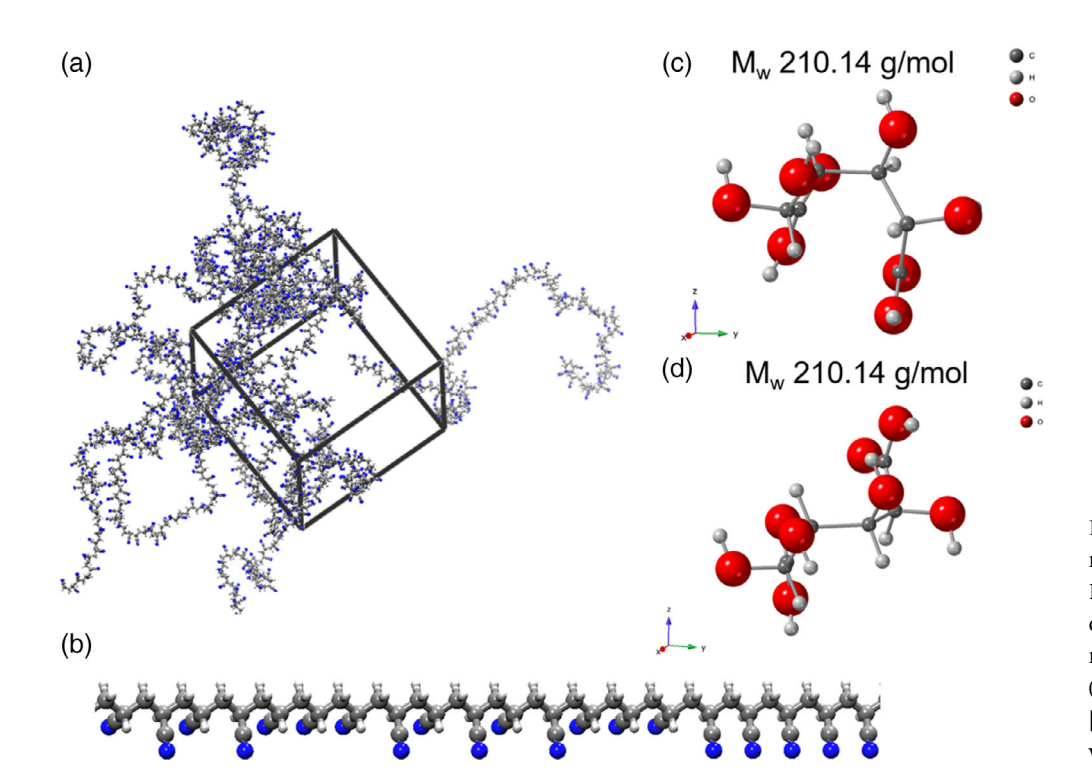


FIGURE 2 Molecular model of feature (a) the initial PAN system, (b) a single chain of atactic PAN, and the molecular structures of the (c) *cis* and (d) *trans* aldaric acids [Color figure can be viewed at wileyonlinelibrary.com]

3 | RESULTS AND DISCUSSIONS

3.1 | Morphology

The SEM images of fiber cross-sections and the longitudinal mounts of fibers are shown in Figure 3. The average effective diameter for each sample is given in Table 1. As evident from Figure 3, the cross-sectional geometry of PAN fibers is kidney-shaped. Consequently, the longitudinal mount of PAN fibers shows an indention that is characteristic of the kidney shape. Additive caused fiber cross-sections to become more oval or circular versus the kidney-shaped PAN fibers. On comparing the effective fiber diameters, PAN and PAN/cis fibers have similar values, which is likely due to the similarities in final draw ratio (36.5 and 38.8 μ m, respectively). Whereas the effective diameter of PAN/trans fiber was the smallest (23.0 μ m), which is in consequence of it having the highest cumulative draw ratio.

3.2 | Processing and structural characteristics of PAN-based fiber

Figure 4 shows 1D diffractometer plots for fully drawn PAN samples. The structural characteristics of PAN fiber against draw ratio are tabulated in Table 2. The polymer chains among PAN fibers tend to arrange in hexagonal packing, having two prominent peaks of [200] along the molecular axis at $2\theta \sim 17^{\circ}$ and [002] at $2\theta \sim 29^{\circ}$. As seen from Table 1, the drawability of as-spun

TABLE 1 Average effective diameter of PAN-based fibers

Samples	Average effective diameter (µm)
PAN	36.5 ± 1.4
PAN/cis	38.8 ± 2.7
PAN/trans	23.0 ± 0.7

PAN/cis and PAN/trans were much greater than that of pure PAN. However, owing to their highly drawn, asspun state of PAN/cis and PAN/trans fibers, they could not be drawn enough through a second stage of drawing in comparison to that of pure PAN fiber. Overall, PAN/trans was drawn the highest amount (to almost ~102 times) versus ~56 X and ~68 X for PAN and PAN/cis, respectively. PAN/trans was of similar crystallinity (~62.8%) to PAN and PAN/cis fibers (at ~64.0% and 63.0%, respectively) although PAN/trans had a vastly higher draw ratio.

The 1-D diffraction patterns were deconvoluted into four major crystalline peaks. In addition to the two hexagonal peaks (at [200] and [002]) as discussed above, two peaks that are smaller and broader in size (at 2θ ~12° and 2θ ~17°) are likely due to the solvation of crystalline PAN and diffraction from off-axis planes (as also seen by Bashir et al. $^{27-30}$). The values of d₂₀₀ and d₀₀₂ do not vary across the samples. As a result, the ratio of d₂₀₀/d₀₀₂ gives an idea of hexagonal perfection among ordered chains of PAN. For all samples, the ratios of d₂₀₀/d₀₀₂ were consistently equal to ~1.73, which is a determining characteristic of hexagonal chain packing.

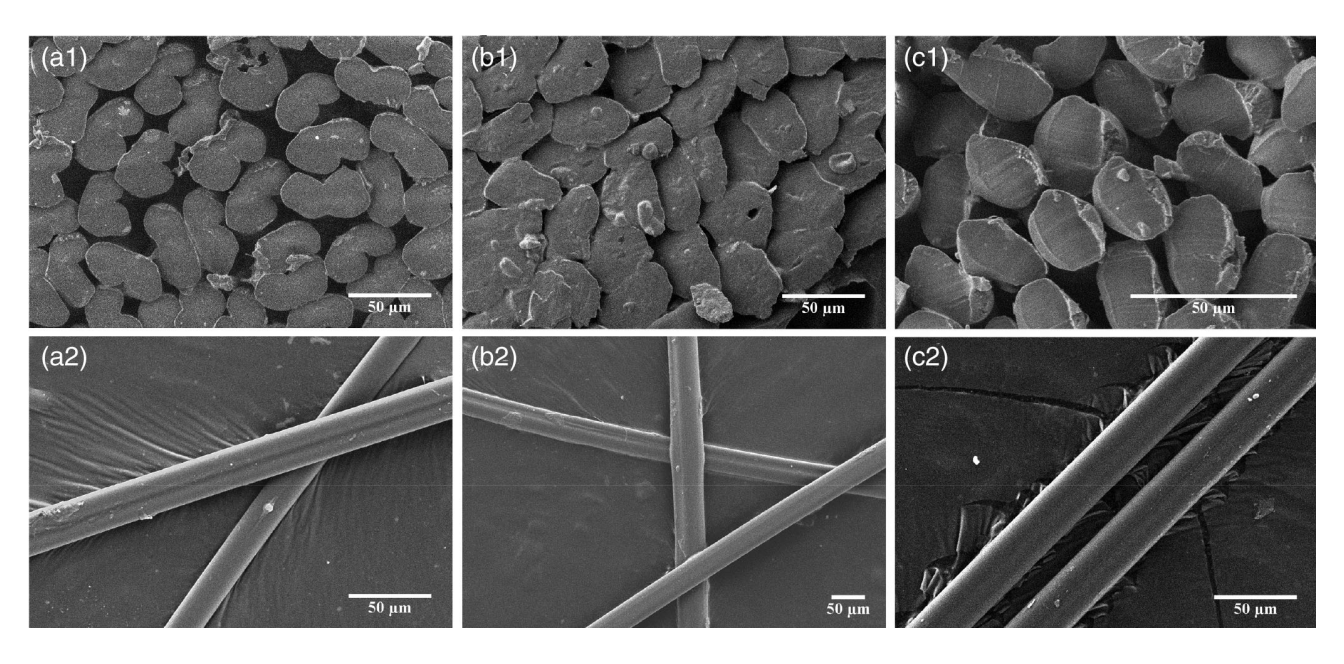


FIGURE 3 Scanning electron microscope (SEM) micrographs of (a) PAN, (b) PAN/cis, and (c) PAN/trans at the (1) fiber cross-section and (2) along the fiber axis

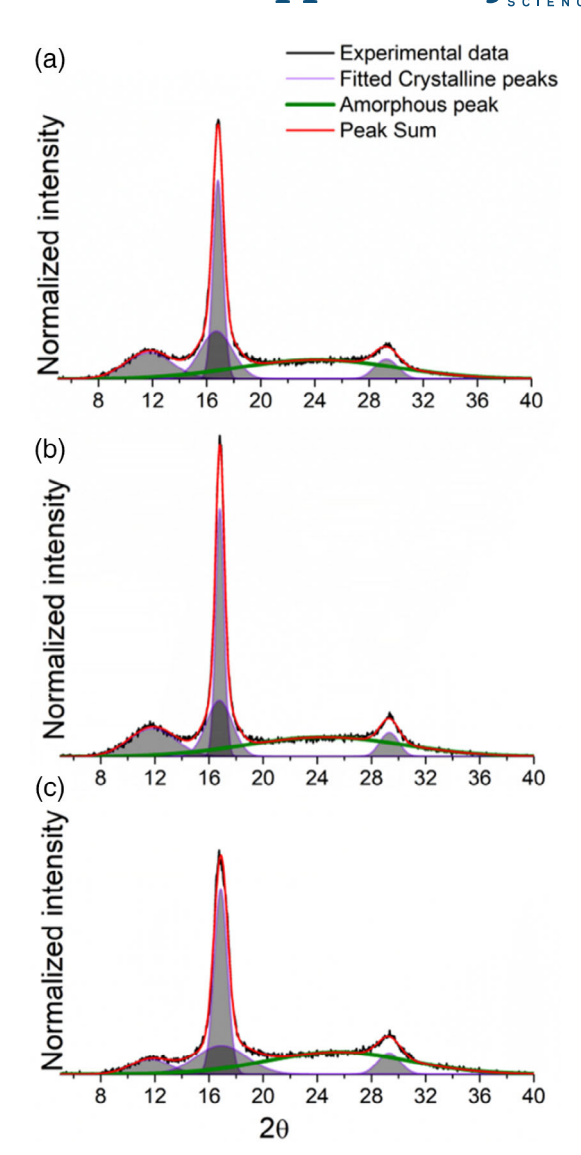


FIGURE 4 1-D WAXD patterns for (a) PAN, (b) PAN/cis, and (c) PAN/trans fibers and their deconvoluted peak fittings are shown [Color figure can be viewed at wileyonlinelibrary.com]

TABLE 2 Processing and WAXD structural parameters for PAN-based fibers

	PAN	PAN/cis	PAN/ trans
As-spun draw ratio	5.6	10.5	15.8
First-stage draw ratio	10	6.5	6.5
Cumulative draw ratio	56.2	68.5	102.7
$d_{[200]}, d_{[002]}(A)$	5.26, 3.05	5.27, 3.04	5.25, 3.04
$d_{[200]}/d_{[002]}$	1.73	1.73	1.73
$\mathrm{FWHM}_{[200]}(^\circ)$	0.9	0.74	1.17
Crystal size _[200] (nm)	8.9	10.8	6.9
Crystallinity (%)	64.0	63.0	62.8

The average crystal size of the [200] peak for fibers containing additive had shown marked differences. The incorporation of trans additive leads to smaller crystals than those observed for pure PAN along the molecular axis, whereas cis additive led to larger crystals along the molecular, even at lower values of draw ratio. A smaller crystallite size along the [200] plane was attributed to the tendency of the trans additive to interfere with the crystalline packing of PAN. Larger crystal size was observed for PAN/cis than for PAN/trans at similar degrees of crystallinity; thus, better crystalline packing was observed with cis than with trans additive.

Molecular modeling 3.3

Differences between $E_1 - E_2$ for PAN/cis and PAN/trans systems are indicative of the energy gaps between initiation and propagation. The slight difference of ~10 kJ/mol between PAN/cis $(E_1 - E_2)$ and PAN/trans $(E_1 - E_2)$ is not clearly understood since both -cis and -trans isomers are chemically similar in terms of the number of hydrogen donors (six in total) and acceptors (eight in total).

MD simulations were carried out to understand how aldaric acids can influence the structure of PAN during processes of fiber spinning and cyclization at a molecular level. Analysis of the radial distribution function (RDF) provides an effective tool for characterizing average atomic structure; experimentally obtained through scattering or diffraction techniques, but also calculable through MD simulations.³¹ A snapshot of molecular assemblies for PAN/cis and PAN/trans are shown in Figure 5a,b. In Figure 5c, the RDF for nitrogen-nitrogen atoms (N-N) of PAN nitrile groups are shown, and the RDF of nitrogen-hydroxyl atoms of the PAN nitrile group with the hydroxyl groups of isomers (e.g., N—OH) are shown. The RDF of N-N pairs exposes the subtle effect of additives on the assembly of PAN nitrile groups. The coordination of nitrogen atoms is slightly higher with the addition of cis additive in the amorphous state compared to trans additive, which closely follows the trend of a neat PAN system. Thus, the cis additive is expected to allow for better packing of nitrile groups during crystallization. The WAXD analysis of fibers, as reported in Table 1, confirms the propensity of PAN/cis to crystallize more readily than without additive or with the trans additive due to its larger crystal size along the [200] molecular axis.

-cis and -trans additive complexes for N—OH both have an identifiable peak at a radial distance (r = 3.24 Å). The coordination frequency g(r = 3.24 Å) for PAN-cis is g

(3.24 Å) = 1.22 and for PAN-trans the value is g (3.24 Å) = 1.06. Further, the second distribution peak for N-OH interactions with PAN/trans occurs at an even longer radial distance of 6.12 Å, where PAN/cis has an N-OH distance of r = 5.88 Å. The snapshot image of the MD provides evidence that -cis additives readily coordinate with the nitrogen atoms of PAN nitrile groups. In contrast, hydroxyl groups of the "extended" trans additive are less coordinated with PAN nitrile groups. The "folded" nature of the cis conformation is believed to render the hydroxyl groups of this aldaric acid more accessible to intramolecular bonding (i.e., N—OH). The cis conformation on average has an orientation of its hydroxyl groups closer to the nitrogen elements of the polymer chain, as seen by the significant difference in peak height at r = 3.24 Å. This gives a plausible reason for the higher crystallite size in PAN/cis than for PAN/trans, evaluated in the previous section. The coordination of cvano groups with hydroxyl groups could lead to better packing in the fiber crystals and therefore higher crystallite sizes were reported for PAN/cis than pure PAN fiber, even though their degrees of crystallinity were similar.

3.4 | Theoretical backdrop in kinetics

The fundamental models of reaction kinetics are shown in this section, ¹⁸ starting with the reaction rate $\left(\frac{d\alpha}{dt}\right)$ in Equation (5),

$$\frac{d\alpha}{dt} = k(T) \cdot f(\alpha) \tag{5}$$

where t is time, k(T) is the temperature-dependent rate constant and $f(\alpha)$ is the reaction model, which is based on conversion α .

The temperature-dependent rate constant is expressed in the form of an Arrhenius relationship per Equation (6),

$$k(T,\alpha) = Ae^{-E_{\alpha}/RT} \tag{6}$$

where *A* is the pre-exponential factor (s⁻¹), E_{α} is the activation energy (J/mol), *T* denotes temperature (K), and *R* is the gas constant (8.314 kJ/mol K).

$$\beta = \frac{dT}{dt} \tag{7}$$

Introducing the term β as the constant heating rate in Equation (6) and the substitution of Equations (6) and (7) in Equation (5) gives

$$\frac{d\alpha}{dT} = \left(\frac{A}{\beta} e^{-E_{\alpha/RT}}\right) \cdot f(\alpha) \tag{8}$$

To evaluate the activation energy of a reaction using the Kissinger method based on peak temperatures, the following equation is used,

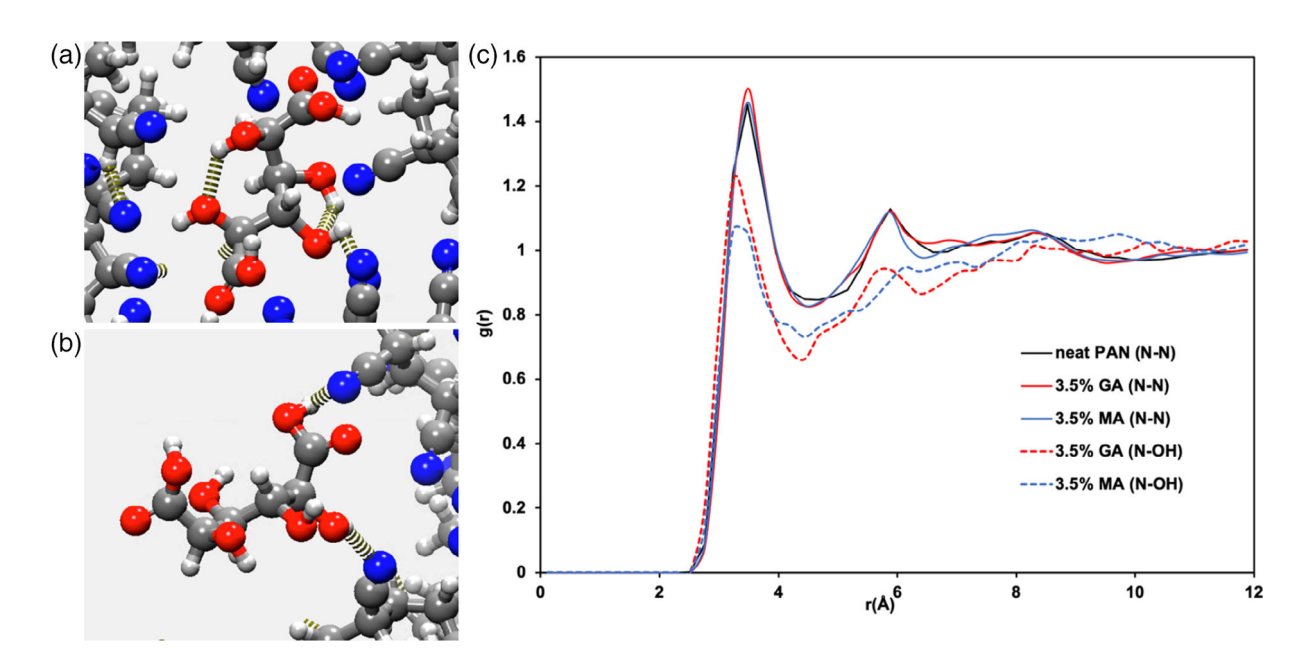


FIGURE 5 Visualization of polymer additive complexes involving the *cis* and *trans* additives using MD simulation: (a) PAN/*cis* complex and (b) PAN/*trans* complex. (c) RDFs for adjacent PAN nitrile groups are denoted by nitrogen-nitrogen (N—N, solid lines). RDFs for nitrogen-hydroxyl groups (N—OH, dotted lines) represent aldaric acid complexes with PAN nitrile groups: PAN/*cis* (red) and PAN/*trans* (blue) [Color figure can be viewed at wileyonlinelibrary.com]

$$\left[\frac{d\ln\frac{\beta}{T_p^2}}{d\left(\frac{1}{T_p}\right)}\right] = -\frac{E}{R} \tag{9}$$

Isoconversional method is based on the governing principle that for a fixed extent of conversion (α), the differential rate of reaction is only a function of temperature.³² This principle is mathematically represented in the form of Equation (10),

$$\left[\frac{d\ln\left(\frac{d\alpha}{dt}\right)}{d\left(\frac{1}{T}\right)} \right] = -\frac{E_{\alpha}}{R}$$
(10)

Kissinger–Akahira–Sunoso (KAS)^{17,33} method is the integral form of the isoconversional approach in Equation (10); KAS is shown in the following Equation (11):

$$\ln\left(\frac{\beta}{T^2}\right) = \ln\frac{AR}{E_{\alpha}g(\alpha)} - \frac{E_{\alpha}}{RT} \tag{11}$$

At constant values of α , plots of $\ln\left(\frac{\beta}{T^2}\right)$ versus $\frac{1}{RT}$ (from Equation 11) yielded linear fits and slope of E_{α} .

3.5 | Proposed mechanism

Proposed mechanisms of 2-step, PAN cyclization is shown in Scheme 1. Since cyclization involves two successive steps, the kinetics of each step is represented by rate constants k_1 and k_2 , with corresponding values of E_1 and E_2 . The cyclization of neat PAN is thermally initiated through the homolytic scission of one of the three C≡N bonds of the nitrile group, 34 as in Scheme 1a. Furthermore, propagation of the cyclization reaction proceeds free-radically through charged centers of adjacent C=N groups. PAN/aldaric acid isomers reactions are illustrated in Scheme 1b; wherein, initiation is assumed to occur via the nucleophilic isomer that anionically attacks the carbon electrophile of the PAN C≡N group. Thus, the carboxylic acid nucleophile is capable of covalently bonding with PAN through its C≡N group. As such, the anion migrates to the nitrogen atom (i.e., $C=N^-$). PAN cyclization propagates anionically across adjacent nitrile units.

The lower values of E_2 (123 and 113 kJ/mol) for PAN/cis and PAN/trans show that the activation energy for anionic propagation has a reduced energy barrier than through free radical propagation. The ionic charge density on nitrogen that is responsible for cyclization is likely lower than the ionic density effects for PAN/trans. As illustrated in our MD simulation results, the interactions between the —OH groups of cis and nitrile groups

of PAN are stronger as compared to that of trans (shown from a smaller distance between them; see Figure 5c. The resultant charge on nitrile groups in the case of cis has more stability and therefore lower reactivity making the anionic propagation slightly less feasible as compared to that of trans. As a result, the higher ionic charge density over nitrogen in the case of PAN/trans may lead to better reactivity and therefore, the lower activation energy for cyclization as compared to that of PAN/cis. Apart from the electrostatic interactions of -OH in aldarics with nitrile groups in PAN, the carboxylic groups of aldarics are solely responsible for forming ionic bonds and an identical activation energy (~180 kJ/mol) of initiation for both PAN/cis and PAN/trans was observed. This shows that the proximity of —OH groups to nitrile groups does not affect the ionic reactivity in the initiation stage in the aldarics incorporated fibers. Therefore, we could easily justify that the results obtained in MD about the proximity of -OH to the nitrile groups still applies if we only consider the -OH contribution from secondary alcohol groups of aldaric acid sugars only. In addition, we could also conclude that the H-bonding between -OH groups in the aldaric acid and cyano groups in PAN possibly sets the tone for the onset of cyclization owing to the proximity of the reactive functional groups in both the species (for PAN/aldaric acid isomers).

3.6 | Kissinger's method based on peak temperatures

Going before the calculation of activation energies based on the isoconversional principle it is important to make the readers understand the common way of evaluating activation energy using peak temperature dependence on the heating rate. Figure 6 shows the Kissinger method based on Equation (9) of evaluating the activation energy for the samples. From the peaks obtained from DSC exotherms, a plot between $\ln\left(\frac{\beta}{T^2}\right)$ and 1/RT has been made for three different heating rates for the samples. The coordinates are specifically taken from the peak point of the exotherms. As seen, PAN has an activation energy of 183.9, while PAN/cis and PAN/trans have an activation energy of 136.5 and 132.6, respectively. The lower activation energy of additive incorporated PAN paves the way and shows that the incorporation of nucleophilic additives has a crucial role to play in reducing the activation energy of the system. However, this method does not give us a clear picture of the whole cyclization process whereby, we are yet to understand how the activation energy differs in the initiation and propagation stages between these precursors. Consequently, the rate of cyclization at the initiation and propagation may be

SCHEME 1 Proposed mechanisms of cyclization among fibers of (a) neat PAN by free radical initiation and (b) PAN/aldaric acid isomer by anionic initiation followed by propagation [Color figure can be viewed at wileyonlinelibrary.com]

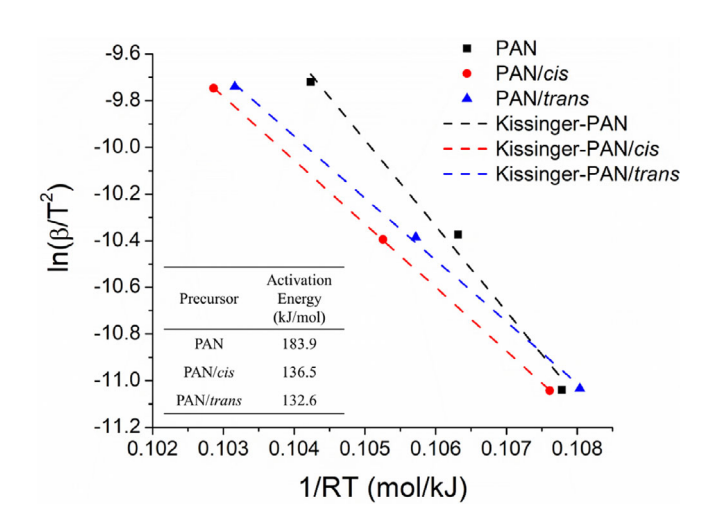


FIGURE 6 Kissinger method used to evaluate the activation energies based on peak temperatures from DSC measurements using Equation (7) [Color figure can be viewed at wileyonlinelibrary.com]

substantially different. To understand the difference in the kinetics between these precursors it is important to look into the isoconversional approach as a tool. The activation energy as a function of conversion can give us important additional insights about our precursors based on different conversion regimes.

3.7 | KAS method

The temperature derivative of the conversion has been plotted in Figure 7 as a function of the temperature

change. Figure 7a3–c3 show plots for PAN, PAN/*cis*, and PAN/*trans* using the KAS method in Equation (10). The values of slope gave the effective activation energy (E_{α}) at specific extents of conversion. Afterward, these values of E_{α} were plotted as a function of α in Figure 8.

The entire conversion regime for the cyclization reaction could be divided mainly into three distinct conversion regimes. The part where the activation energy drops monotonically up to a conversion of 0.6 has been attributed to a kinetic-controlled regime (autocatalytic). This is the region where the autocatalytic activity in the fiber happens. Beyond this regime, activation energy attains a plateau, and this could be mainly caused due to primarily a single class of propagation reaction taking place (see Scheme 1). Although it is understood that to characterize a kinetic system evaluation of pre-exponential factor is important, the discussions on this aspect do not support our discussion on the use of additives in catalyzing the cyclization process. Eventually, the activation energy beyond the conversion of 0.85 was seen to fall off, and the prime reason that could be attributed to is the diffusion limitation within the fibers that led to reaction termination. These diffusive limitations have also been discussed previously by Vyazovkin et al.¹²

3.8 | Autocatalytic cyclization reaction

The E_{α} for PAN follows a monotonic drop from 866.1 to 175.8 kJ/mol at $\alpha = 60\%$. Subsequently, E_{α} plateaus between $60\% < \alpha < 85\%$. On the contrary, $E_{\text{a.onset}}$ values

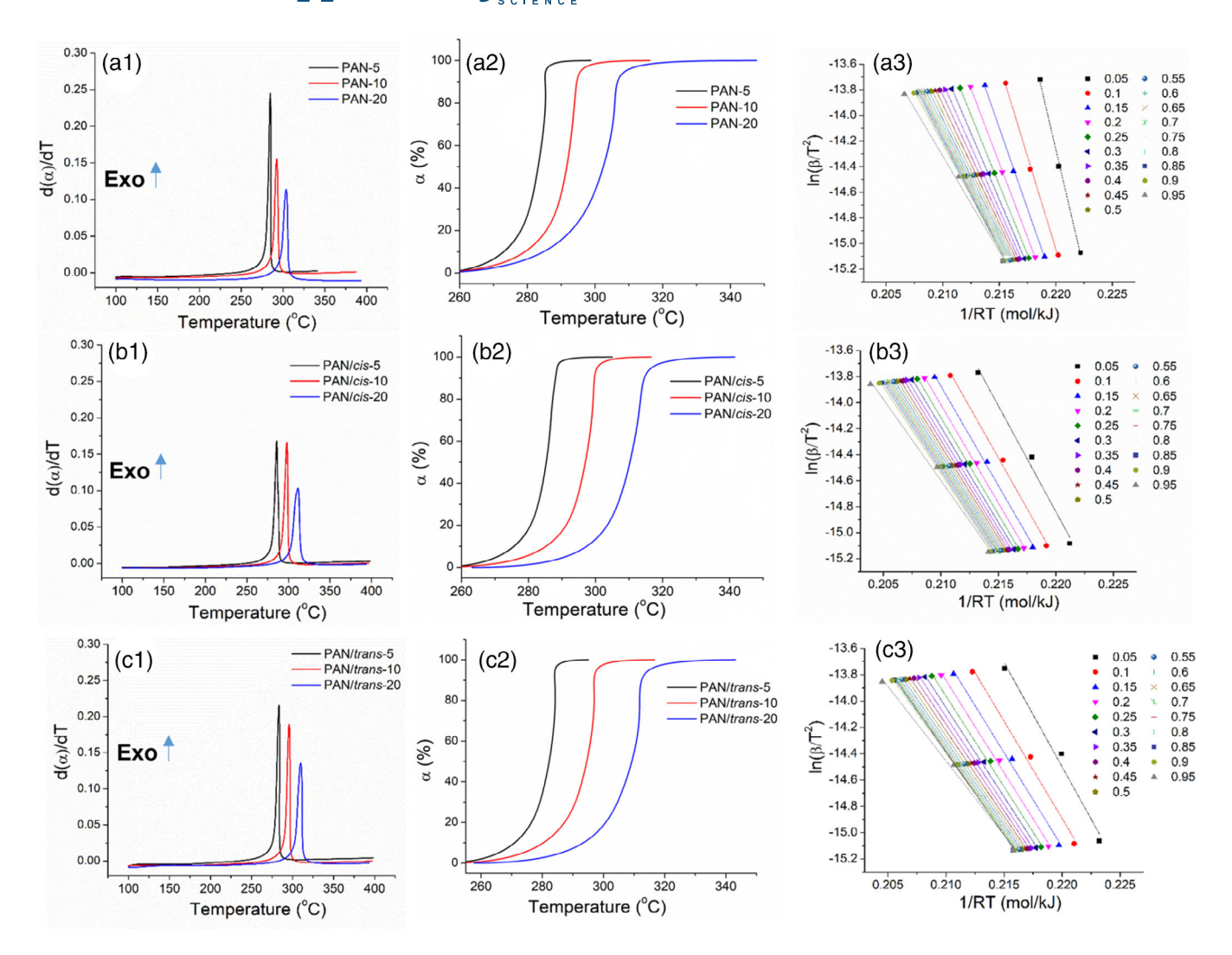
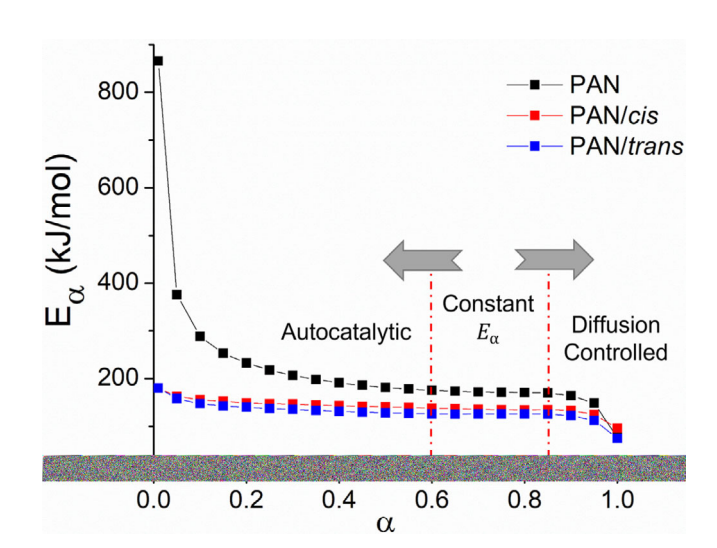


FIGURE 7 Thermal profiles for (a) PAN, (b) PAN/*cis*, and (c) PAN/*trans* are shown for (1) temperature differential of conversion (a) as a function of temperature at heating rates of 5, 10, and 20°C/min, (2) conversion versus temperature, and the slope of KAS plots were evaluated for conversion-dependent activation energy (E_{α}) [Color figure can be viewed at wileyonlinelibrary.com]

for PAN/cis and PAN/trans were considerably lower than that of neat PAN fiber, and E_{α} values depreciated at a much slower rate with conversion than for PAN. $E_{\rm a,onset}=180.8$ kJ/mol for PAN/cis and PAN/trans decreased to 138.4 and 126.3 kJ/mol, respectively at $\alpha=60\%$. The major difference between the kinetics of PAN with and without additive lies in the magnitude of E_{α} , especially at the onset of the reaction.

The fact that PAN fibers have such a high onset value for activation energy is a challenge that has generally been addressed by copolymerizing AN with monomers having nucleophilic groups; such as IA or MAA up to 5 mol% AN. Otherwise, cyclization among PAN homopolymer is initiated free radically.³⁵ Both IA and MAA comonomers are internal initiators for the initiation of PAN cyclization ionically.³⁴ Differences between $E_{a,onset}$ for neat PAN versus PAN with additive can be attributed

to the nucleophilic diacid groups in the cis and trans additives. Thus, the high $E_{a,onset}$ barrier for PAN was significantly decreased through the use of aldaric acid isomers, which behaved as external initiators for PAN cyclization. Also from Figure 7a1-c1, it can be seen that the incorporation of these additives does not lead to a drop in the onset of cyclization temperature. As demonstrated in Figure 8, it is not reasonable to define cyclization as a single-step reaction, but rather as a sequence of reaction models. Differences among $E_{a,onset}$ for PAN, PAN/cis, and PAN/trans allows us to conclude that the kinetics of initiation can also differ in terms of k, E_{α} , and $g(\alpha)$. This E_{α} regime of $\alpha < 0.6$ was empirically determined to fit the model for autocatalytic reaction, as also observed for the epoxy-amine curing reported by Vyazovkin and Sbirrazzuoli. ¹² In both cases, E_{α} drops monotonically before plateauing to steady-state.



The integration of Equation (10) where $\frac{d\alpha}{dt} = (k_1 + \alpha^m k_2)(1-\alpha)^n$, was arranged to determine the kinetic models for PAN cyclization, as observed for $E(\alpha)$ values in Figure 9. Equation (12) represents the model that was fitted using Origin Pro 8.5 for activation energies E_1 and E_2 , rate constant ratios k_1/k_2 , and m: 37

$$E_{\alpha} = \frac{\left(\frac{k_1}{k_2}\right)E_1 + \alpha^m E_2}{\left(\frac{k_1}{k_2}\right) + \alpha^m} \tag{12}$$

The values of E_1 and E_2 correspond to the activation energies of each class of reaction while, k_1/k_2 is the ratio of the rate constants between each class of reactions, as per Scheme 1. The model illustrated in Equation (12) enables the fitting of experimental data using E_α , where $\alpha \leq 0.6$ and $E_2 \leq E_\alpha \leq E_1$. The model-fitting parameters are tabulated in Table 3.

The cyclization process can be aptly understood as a function of two reactions in series. As evident from Table 3, the values of E_1 and E_2 correspond to the individual steps in the cyclization process. Neat PAN fiber had a much higher value of E_1 (947 kJ/mol) than was seen for the E_1 values of PAN/cis and PAN/trans for the initiation of cyclization. This value is significantly higher than the value of E_2 (175.8 kJ/mol), which is the activation energy for propagation for PAN. Our E_2 for PAN (MAA = 0.5%) closely resembles the activation energy of cyclization for PAN-MAA fiber evaluated using peak temperature, where 183.1 kJ/mol was reported for MAA comonomer at 4% of PAN by Liu et al. 9 Further, Xiao et al. reported 190 kJ/mol for PAN/IA and PAN/MA

systems that were evaluated based on peak DSC exotherms. 9,38 Such a high value of activation energy for initiation (947 kJ/mol) is one of the greatest demerits of using PAN devoid of an adequate proportion of internal or external initiators for stabilization. In the case of PAN/cis and PAN/trans, the activation energy of initiation drastically drops to 191 and 188 kJ/mol, which is almost five times lower than for PAN fiber. This decrease in E_1 suggests the addition of aldaric acid can externally catalyze the kinetics of cyclization. MD simulations

Sample	k_1/k_2	E_1 (kJ/mol)	E_2 (kJ/mol)	m	R^2
PAN	0.0037	947	175	1.60	0.989
PAN/cis	0.228	191	123	0.65	0.990
PAN/trans	0.15	188	113	0.81	0.991

TABLE 3 Fitting parameters for PAN cyclization is based on E_{α} autocatalytic model represented by Equation (12)

TABLE 4 Comparison of the activation energy values evaluated using the Kissinger method and pre-exponential factor for cyclization to some of the standard values collected from the literature

Sample	Nucleophile group fraction	E (kJ/mol)	Reference
Polyacrylonitrile (composites)	-	142.8	40
Poly(acrylonitrile-acrylic acid)	3.1 mol%	184.8	23
Poly(acrylonitrile-methacrylic acid)	2.6 mol%	123.3	23
Poly(acrylonitrile-itaconic acid)	4.4 mol%	109.1	23
Poly(AN-MAA)	5 mol%	107.1	3
Amino CNT-PAN (composites)	1%	154.9	40
Poly(AN-IA-MAA) ^a	1.2: 6%	114.3	41
Poly(AN-IAA)	NA	159.1	42
Poly(AN-MAA)	4 mol%	183.1	9
Poly(AN-IA) powder	3 mol%	103.7	34
$\mathbf{PAN}^{\mathrm{b}}$	0.5 mol%	183.9	This work
PAN ^b /cis	$0.5+1.8~\mathrm{mol\%}$	136.5	This work
PAN ^b /trans	$0.5+1.8~\mathrm{mol\%}$	132.6	This work

Note: Measurement is made based on peak temperature positions using the Kissinger method.

revealed that the -OH group from the aldaric acid isomers take part in H-bonding with pendant cyano groups of PAN which might become the driving force for the sugar molecules to be at the vicinity of the electrophilic C-center of the cyano groups. As seen from Scheme 1b, the H-bonding of the cyano group with the carboxylate group of aldaric acid isomers played a key role in the cyclization. This H-bonding is the plausible cause for the generation of more electrophilic C-centers on the cyano groups. The carboxylate groups of aldaric isomers act as positional initiators that enable the carboxylate ions to attack the electrophilic C-center and start the cyclization reaction (as evident from lower E_1). The behavior is similar to the H-bonding catalysis that relies on the use of Hbonding interactions to accelerate and control organic reactions.³⁹ Corresponding values of E_2 , as evaluated for PAN/cis and PAN/trans, are significantly lower than that of PAN.

Based on values of k_1/k_2 , the rate of PAN initiation $(k_1/k_2 = 0.0037)$ is significantly lower than that of PAN/cis $(k_1/k_2 = 0.228)$ and PAN/trans $(k_1/k_2 = 0.15)$. These values show that PAN has a rate constant for initiation rate (k_1) that is significantly lower than that of

propagation (k_2) . The behavior for PAN cyclization completely changes upon the introduction of aldaric acid additives, for which k_1/k_2 increased by almost two orders of magnitudes. The k_1/k_2 for PAN/cis and PAN/trans are of the same order of magnitude and are more similar; this is primarily because of similarities between their chemical structures. A very low value for k_1/k_2 coupled with a very high E_1 for PAN reconfirms that PAN fibers require catalysis to overcome the high energy barrier for initiation.

The value of m corresponds to a fitting parameter for the kinetic model, which corresponds to the steepness of the curve. PAN has the highest value of m=1.6 because the E_{α} falls steeply with the conversion from $E_{\alpha, \text{onset}}$. This fall is due to the autocatalytic nature of cyclization where the active free radical propagates cyclization juxtaposed to free radical initiation through bond scission. While lower values of m=0.65 and m=0.8 for PAN/cis and PAN/trans, respectively, show how E_{α} does not fall as steep up to $\alpha=0.6$ in comparison to PAN. As shown in Table 3, differences between E_1 and E_2 for initiation and propagation, respectively, are similar in the cases of PAN/cis and PAN/trans fibers. Since E_2 effectively would

awt % in solution.

^b0.5 mol% MAA.

indicate the value of E during reaction propagation, its lower value in the case of PAN/cis and PAN/trans would indicate the better kinetics of the ionic propagation as compared to the free-radical propagation in the case of PAN. Practically, the value of E shows the extent to which the values of E_1 and E_2 differ. The higher the difference between these two values, the more autocatalytic the nature would be and so would be the value of E.

3.9 | Comparison with literature

Table 4 summarizes values of activation energy as recorded in the literature for cyclization. Comparable activation energy values for PAN/cis and PAN/trans systems were seen to that of some PAN copolymers, where an appreciable amount of nucleophilic comonomer was used. The PAN-MAA copolymer study, as reported by Bahrami et al., possessed 2.6 mol % comonomer; an E=123.3 kJ/mol was seen. This work has shown competitive values of activation energy when using additive; $E_{\rm a,onset}$ values were 132.6–136.5 kJ/mol) at 2.3% of the nucleophilic initiator.

4 | CONCLUSION

The study proposes the use of aldaric acid isomers as viable initiators for PAN fiber cyclization. This study showed the potential to lower E_{α} with current PAN homo and copolymers using additives. This work has demonstrated that the autocatalytic model can be used to evaluate reaction kinetics of PAN cyclization from DSC data. The results show the decay of activation energies of the fibers signifying a higher activation barrier for initiation of the reaction. Non-additive incorporated PAN fibers suffer from poor activation energy at the start of reaction while PAN/cis and PAN/trans significantly catalyze the initiation in the cyclization process. The sugar isomers act as positional initiators that effectively initiate the nucleophilic cyclization reaction juxtaposed to a thermal initiated free-radical cyclization reaction in PAN. The overall reaction was characterized using model-free a isoconversional approach along with the activation energy evaluated using the Kissinger method based on peak temperatures. The study revealed that the modelfree isoconversional approach was capable of deducing the reaction mechanism of the system in contrast to the simple Kissinger method based on peak temperatures that yield a single value of activation energy for a reaction process. The entire activation energy regime was divided into three zones namely, autocatalytic controlled regime, constant activation energy regime, and diffusioncontrolled regime. A model for autocatalysis was applied to the autocatalytic regime, where the activation energy showed a gradual drop with conversion ($\alpha \le 0.6$). The autocatalytic reaction model showed a five times improvement in the activation energy of initiation for PAN/cis and PAN/trans. As a consequence, it was seen that the ratio of the rate constants for initiation to that of propagation was enhanced by almost two orders of magnitude when compared to PAN fibers without additive. The lower activation energy specifically during the initiation state for our additive-based system would lead to lower energy requirements during non-isothermal cyclization. A higher value for the rate constant ratio of the PAN/cis and PAN/trans systems signifies cyclization would initiate at faster rates as compared to that of PAN fibers. MD simulations showed that the -OH groups from aldaric acid isomers H-bonded with the cyano groups of PAN led to kinetically favorable ionic initiation of cyclization. MD simulation results were also used to conclude that the cis GA hydroxyl groups were in closer proximity to PAN nitrile groups than MA hydroxyl groups with PAN. This is the most probable reason for slight differences in activation energy between the two additive incorporated precursors. The values of activation energy for PAN/cis and PAN/trans compared quite well with the existing activation energies for PAN copolymers. It may be concluded from this study that strong intermolecular forces can be used to cause external molecules and additives to promote or interfere with cyclization.

ACKNOWLEDGMENTS

The authors D.B. and E.F. would like to acknowledge the Chancellor's Innovation Fund for the financial support provided for some of this work. This work was performed in part at the Chemical Analysis & Spectroscopy Lab, Department of Forest Biomaterials at North Carolina State University. The authors would also like to thank and acknowledge computing resources provided on Henry2; a high-performance computing cluster operated by North Carolina State University. The authors would also like to acknowledge NSF NRT on Data-Enabled Science and Engineering of Atomic Structures (DGE-1633587). In addition, the authors sincerely acknowledge the assistance of Kalion, Inc. in supplying glucaric acid as one of the additives for our systems.

CONFLICT OF INTEREST

The authors declare no financial/commercial conflicts of interest.

ORCID

Debjyoti Banerjee https://orcid.org/0000-0001-7130-734X

REFERENCES

- [1] Y. Liu, S. Kumar, Polym. Rev. 2012, 52, 234.
- [2] C. D. Warren, Carbon Fiber Precursors and Conversion 2016. https://www.energy.gov/sites/default/files/2016/09/f33/fcto_ h2_storage_700bar_workshop_3_warren.pdf
- [3] E. Fitzer, D. J. Müller, Carbon 1975, 13, 63.
- [4] I. Noh, H. Yu, J. Polym. Sci., Part B: Polym. Lett. 1966, 4, 721.
- [5] K. Morita, H. Miyachi, T. Hiramatsu, Carbon 1981, 19, 11.
- [6] G. L. Collins, N. W. Thomas, G. E. Williams, Carbon 1988, 26, 671.
- [7] J. N. Hay, J. Polym. Sci. Part A-1 Polym. Chem. 1968, 6, 2127.
- [8] S. S. Belyaev, I. V. Arkhangelsky, I. V. Makarenko, Thermochim. Acta 2010, 507–508, 9.
- [9] H. C. Liu, A. T. Chien, B. A. Newcomb, A. A. Bakhtiary Davijani, S. Kumar, *Carbon* 2016, 101, 382.
- [10] J. D. Moskowitz, W. Jacobs, A. Tucker, M. Astrove, B. Harmon, Polym. Degrad. Stab. 2020, 178, 109198.
- [11] S. Vyazovkin, C. A. Wight, Thermochim. Acta 1999, 340– 341, 53.
- [12] S. Vyazovkin, N. Sbirrazzuoli, Macromolecules 1996, 29, 1867.
- [13] S. Vyazovkin, J. Therm. Anal. Calorim. 2006, 83, 45.
- [14] H. L. Friedman, J. Polym. Sci., Part C: Polym. Symp. 1964, 6, 183.
- [15] J. H. Flynn, L. A. Wall, J. Res. Natl. Bur. Stand. Sect. A: Phys. Chem. 1966, 70A, 487.
- [16] T. Ozawa, Bull. Chem. Soc. Jpn. 1965, 38, 1881.
- [17] H. E. Kissinger, Anal. Chem. 1702, 1957, 29.
- [18] G. Mishra, T. Bhaskar, Bioresour. Technol. 2014, 169, 614.
- [19] B. Janković, B. Adnadević, J. Jovanović, Thermochim. Acta 2007, 452, 106.
- [20] Y. Hu, Z. Wang, X. Cheng, C. Ma, RSC Adv. 2018, 8, 22909.
- [21] Y. Xue, J. Liu, J. Liang, Polym. Degrad. Stab. 2013, 98, 219.
- [22] A. K. Gupta, D. K. Paliwal, P. Bajaj, J. Macromol. Sci. Part C 1991, 31, 1.
- [23] S. Hajir Bahrami, P. Bajaj, K. Sen, J. Appl. Polym. Sci. 2003, 88, 685.
- [24] E. N. J. Ford, S. K. Mendon, S. F. Thames, J. W. Rawlins, J. Eng. Fibers Fabr. 2010, 5, 155892501000500.
- [25] S. L. Mayo, B. D. Olafson, W. A. Goddard, J. Phys. Chem. 1990, 94, 8897.

- [26] B. A. Luty, W. F. Van Gunsteren, J. Phys. Chem. 1996, 100, 2581.
- [27] Z. Bashir, S. P. Church, D. M. Price, Acta Polym. 1993, 44, 211.
- [28] Z. Bashir, Polymer 1992, 33, 4304.
- [29] Z. Bashir, J. Polym. Sci. Part B: Polym. Phys. 1994, 32, 1115.
- [30] Z. Bashir, J. Mater. Sci. Lett. 1993, 12, 1526.
- [31] J. M. Pires, O. V. de Oliveira, L. C. G. Freitas, E. A. S. da Filho, A. R. Prado, *Comput. Theor. Chem.* **2012**, 995, 75.
- [32] S. Vyazovkin, N. Sbirrazzuoli, Macromol. Rapid Commun. 2006, 27, 1515.
- [33] A. C. R. Lim, B. L. F. Chin, Z. A. Jawad, K. L. Hii, Proc. Eng. 2016, 148, 1247.
- [34] Q. Ouyang, L. Cheng, H. Wang, K. Li, Polym. Degrad. Stab. 2008, 93, 1415.
- [35] Q. He, P. Zhou, J. Hao, C. Lu, Y. Liu, ACS Omega 2019, 4, 11346.
- [36] M. E. Ryan, A. Dutta, Polymer 1979, 20, 203.
- [37] S. Vyazovkin, Macromol. Rapid Commun. 2017, 38, 1.
- [38] S. Xiao, W. Cao, B. Wang, L. Xu, B. Chen, J. Appl. Polym. Sci. 2013, 127, 3198.
- [39] R. R. Knowles, E. N. Jacobsen, Proc. Natl. Acad. Sci. USA 2010, 107, 20678.
- [40] L. Quan, H. Zhang, L. Xu, J. Therm. Anal. Calorim. 2015, 119, 1081.
- [41] Y. Liu, Y. Xue, H. Ji, J. Liu, J. Appl. Polym. Sci. 2020, 137, 48819.
- [42] Y. Hou, T. Sun, H. Wang, D. Wu, J. Mater. Sci. 2008, 43, 4910.

SUPPORTING INFORMATION

Additional supporting information may be found in the online version of the article at the publisher's website.

How to cite this article: D. Banerjee,

H. Dedmon, F. Rahmani, M. Pasquinelli, E. Ford, J. Appl. Polym. Sci. **2022**, 139(11), e51781. https://doi.org/10.1002/app.51781